

Functional Expression of Murine V2R Pheromone Receptors Involves Selective Association with the M10 and M1 Families of MHC Class Ib Molecules

Jennifer Loconto,^{1,4,6} Fabio Papes,^{1,4} Ernie Chang,¹ Lisa Stowers,^{1,5} Elys P. Jones,² Toyoyuki Takada,^{3,7} Attila Kumánovics,² Kirsten Fischer Lindahl,^{2,3} and Catherine Dulac^{1,*}

¹Department of Molecular and Cellular Biology
Howard Hughes Medical Institute
Harvard University
Cambridge, Massachusetts 02138

²Center for Immunology
³Howard Hughes Medical Institute
University of Texas Southwestern Medical Center
Dallas, Texas 75390

Summary

The vomeronasal organ (VNO) of the mouse has two neuronal compartments expressing distinct families of pheromone receptors, the V1Rs and the V2Rs. We report here that two families of major histocompatibility complex (MHC) class Ib molecules, the M10 and the M1 families, show restricted expression in V2R-expressing neurons. Our data suggest that neurons expressing a given V2R specifically co-express one or a few members of the M10 family. Biochemical and immunocytochemical analysis demonstrates that in VNO sensory dendrites M10s belong to large multi-molecular complexes that include pheromone receptors and β2-microglobulin (β2m). In cultured cells, M10s appear to function as escort molecules in transport of V2Rs to the cell surface. Accordingly, β2m-deficient mice exhibit mislocalization of V2Rs in the VNO and a specific defect in male-male aggressive behavior. The functional characterization of M10 highlights an unexpected role for MHC molecules in pheromone detection by mammalian VNO neurons.

Introduction

The vomeronasal organ (VNO) of mammals plays an essential role in the detection of pheromones, a discrete class of chemical cues released by animals that elicit various neuroendocrine changes and triggers genetically preprogrammed behaviors such as mating and territorial defense. How is the information about the sex, and the reproductive and social status of conspecifics detected by the VNO and translated into appropriate behavioral and neuroendocrine responses? Genetic ablation of VNO function by gene targeting of the TRP2 ion channel leads to a striking behavioral phenotype in

the mutant line, which illuminates the physiological role of the vomeronasal system in the mouse (Stowers et al., 2002; Leybold et al., 2002). Male mice deficient in TRP2 expression fail to display male-male aggression and engage in sexual behavior with conspecifics of both sexes. Thus, we have proposed that a major function of the VNO is to ensure the gender specificity of male mouse behavior by providing the brain with sensory cues essential for sex discrimination.

How is the sex of a conspecific recognized by the VNO? Differential screening of cDNA libraries constructed from individual rodent VNO neurons has led to the isolation of two large and independent families of VNO-specific G protein-coupled receptors (GPCRs), the V1R and V2R vomeronasal receptors, likely to represent the mammalian pheromone receptors (Dulac, 2000). V1Rs and V2Rs are both unrelated to each other and to the olfactory receptors (ORs). Each family is comprised of 100–200 putative pheromone receptor genes that are expressed in two spatially segregated populations of VNO sensory neurons. Neurons lining the luminal (or apical) half of the VNO neuroepithelium co-express V1Rs and the G protein α subunit Gαi2. In contrast, the basal half of the VNO epithelium contains neurons that are V2R- and Gαo-positive. VNO sensory fibers reaching the accessory olfactory bulb (AOB) remain segregated according to their origin from the apical or basal sides of the VNO, with Gαo-positive fibers projecting to the posterior half of the AOB and Gαi2-positive fibers reaching the anterior portion of the AOB (Halpern et al., 1998). The expression of molecularly divergent pheromone receptors by these two spatially segregated populations of sensory neurons may indicate that the vomeronasal system comprises two separate functional units in order to detect and process pheromone signals.

How is the diversity and specificity of the pheromone response accomplished? It is very likely that, as in insects and fish, pheromonal recognition in rodents involves the activation of multiple receptors by specific cocktails of chemical cues rather than the action of single pheromonal compounds (Sorensen et al., 1998). Because both pheromone receptor families are comprised of several hundred genes each, it might be difficult to determine directly, at least as a first step, which precise subset of V1R and V2R receptors contribute to a given behavior or endocrine change. Accordingly, the genetic ablation of a small subset of V1Rs generates a modest but complex behavioral phenotype that is difficult to interpret (Del Punta et al., 2002b). Instead, we reasoned that significant information about the molecular and physiological nature of the VNO response may be obtained by in depth analysis of each V1R-positive and V2R-positive neuronal subpopulations, in turn permitting the direct functional analysis of specific receptor subsets.

A subtractive differential screening of cDNA libraries prepared from individual neurons expressing a V1R or a V2R pheromone receptor resulted in the isolation of large sets of genes with restricted expression patterns in the basal and apical portions of the VNO (Supplemental

*Correspondence: dulac@fas.harvard.edu

⁴These authors contributed equally to this work.

⁵Present address: The Scripps Research Institute, Department of Cell Biology, ICND 222, La Jolla, California 92037.

⁶Present address: Anthony Nolan Research Institute, Royal Free Hospital, London NW3 2QG, United Kingdom.

⁷Present address: Laboratory Animal Science, The Tokyo Metropolitan Institute of Medical Science, 3-18-22, Honkomagome, Bunkyo-ku, Tokyo 113-8613, Japan.

Figure S1 available at <http://www.cell.com/cgi/content/full/112/5/607/DC1>). We report here the characterization of two families of MHC class Ib genes, called *M10* and *M1*, with exclusive expression in the basal zone of the VNO. The molecular, cellular, and functional properties of *M10* and *M1* molecules provide unexpected insights into the process of pheromone detection in mammals.

Results

Characterization of the *M10* Family of MHC Molecules

*Identification of *M10* Transcripts in the Rat and Mouse VNO*

A subtractive cloning strategy performed in the rat between amplified single-cell cDNAs originating from individual $\text{G}\alpha\text{i}2$ - and $\text{G}\alpha\text{o}$ -positive VNO neurons led to the isolation of various cDNA clones with restricted expression in the basal or apical zones of the neuroepithelium (Supplemental Figure S1 available at above website). Among the various transcripts identified, clone 144 attracted our attention based on its restricted expression in the basal zone of the VNO, its absence from the main olfactory epithelium (MOE), and its intriguing sequence homology to nonclassical MHC class I (or class Ib) genes. Because the mouse is more amenable to molecular biology than the rat, we pursued further analysis in that species. We cloned the mouse homolog of clone 144 which appeared identical to *M10.7*, a member of the *M10* family of class Ib genes whose chromosomal location and genomic sequence has been reported previously (Arepalli et al., 1998; Jones et al., 1999; Takada et al., 2003).

*The *M10* Genomic Locus*

The *M10* family is clustered in a 500 kb region at the telomeric end of the mouse MHC, the *H2* locus. The family is composed of eight homologous genes, named *M10.1* to *M10.8*, of which *M10.4* and *M10.6* are pseudogenes (Figure 1A). Our search for *M10* transcripts in a mouse VNO cDNA library identified six *M10* family members (*M10.1*, *M10.2*, *M10.3*, *M10.5*, *M10.7*, and *M10.8*), present at a frequency of 0.1% of expressed genes. This makes *M10* one of the most highly expressed group of genes in the VNO, with a level of expression comparable to that of pheromone receptor genes. In contrast, we were unable to isolate transcripts of *M10.4* and *M10.6*, which do not have complete open reading frames.

Within the *H2* locus, the *M10* family is arranged in two clusters surrounding the *M1* family of MHC class Ib genes (Figure 1A). Members of the *M1* family share 76% amino acid identity and are the closest relatives of the *M10* family (Arepalli et al., 1998; Takada et al., 2003; Kumánovics et al., 2003). Three of the five *M1* family members (*M1*, *M9*, and *M7.2*) are predicted to code for functional proteins, and their transcripts were also identified in the VNO.

In situ hybridization using a mixture of all *M10* probes or individual *M10* probes shows that *M10* genes are expressed by a large subset of cells in the $\text{G}\alpha\text{o}$ -positive, V2R-positive basal zone of the VNO (Figure 1B). The likely cross-hybridization of RNA probes representing each individual *M10* member to transcripts of other *M10s* limits the ability to directly assess the ratio of cells

expressing a specific *M10* gene (see below). In contrast, *M1* and *M9* are expressed by only 0.1–1% of the VNO neurons, displaying a pattern of expression in the basal VNO neuroepithelium that mirrors that of a single pheromone receptor (Figure 1B).

Expression of MHC Accessory Molecules in the VNO

The presence of *M10* transcripts in the VNO raised the possibility that other proteins usually found in association with MHC molecules, such as $\beta 2$ -microglobulin ($\beta 2\text{m}$) and TAP-1 and -2, may be expressed there as well. $\beta 2\text{m}$ interacts with all classical and most nonclassical MHC to provide a stable 3-dimensional structure at the cell surface. TAP-1 and -2 are subunits of a heterodimeric member of the ATP binding cassette (ABC) family of transporters, responsible for transporting peptides into the ER to be loaded onto newly synthesized MHC class I heavy chains. In situ hybridization revealed that *B2m* is expressed in the basal VNO neurons in a pattern similar to that of *M10* (Figure 1B). In contrast, although we could amplify TAP sequences from VNO cDNA, in situ hybridization experiments on VNO sections failed to reveal expression of either gene at a detectable level (not shown).

Tissue Distribution

In situ hybridization with *M10* RNA probes on sections from a large variety of neuronal and non-neuronal tissues could not identify any detectable expression of the *M10* family outside the VNO (not shown). Similarly, in RT-PCR experiments performed on a comprehensive series of tissues (Figure 1C) using generic primers for the *M10* genes, the VNO appeared to be the exclusive source of *M10* transcripts, thus confirming the original difficulty in locating a source of expression of *M10*, *M1*, and *M9* in the mouse (Arepalli et al., 1998).

*Sequence Analysis of *M10* Proteins*

The *M10* family shares many structural characteristics with classical MHC molecules, including the four invariably conserved cysteines that form disulphide bridges in the $\alpha 2$ and $\alpha 3$ domains (Figure 2A). A key feature of MHC class Ia molecules is the presence of a peptide binding pocket, formed by the $\alpha 1$ and $\alpha 2$ domains and used to present intracellularly derived peptides of 8 to 10 residues to TCR complexes at the surface of cytotoxic T lymphocytes. This peptide binding cleft is made out of an eight-stranded antiparallel β sheet topped by two α helices (Figure 2B) and is positioned on top of the immunoglobulin-like constant $\alpha 3$ domain bound to $\beta 2\text{m}$. The peptide binding groove can be subdivided into six pockets A, B, C, D, E, and F. The N terminus of a bound peptide fits into the A pocket, where it is held by hydrogen bonds to four conserved tyrosines, Y7, Y59, Y159 and Y171; whereas the mainchain atoms of the peptide C terminus interact with Y84, T143, K146, and W147 at the other end of the groove. Peptide side chains lodge into the B, C, D, E, and F pockets.

M10 is missing four of the residues that are generally conserved for peptide interactions (Y7, Y84, T143, and K146). Furthermore, residue 167 is a tryptophan in all class Ia molecules, positioned along the edge of the A pocket of the peptide binding groove. In all *M10s*, this residue has been replaced with an arginine. The same replacement is found in *Fcgtr*, also known as *FcRn*, the neonatal Fc receptor, where that arginine points into

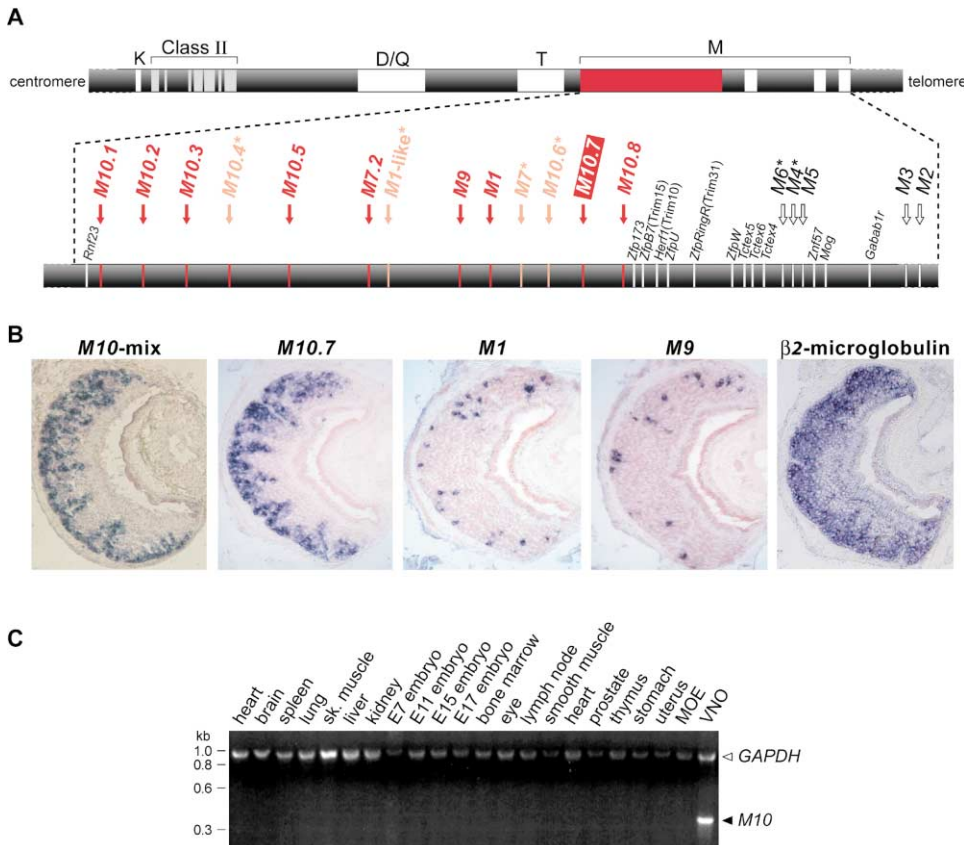


Figure 1. Exclusive Expression of Nonclassical Class I MHC Molecules in the VNO

(A) Map of the *H2-M* region on chromosome 17 (adapted from Takada et al., 2003). Six out of eight *M10* family genes and three out of five *M1* family genes (indicated in red), are likely to generate functional transcripts. Pseudogenes are indicated in orange with an asterisk. Adjacent *H2-M* class I and unrelated genes not expressed in the VNO are shown in black, with an asterisk for pseudogenes.
(B) Expression of *M10* and *M1* transcripts in the VNO. RNA probes representing a mix of all *M10* transcripts label large subsets of basal VNO neurons, while the *M10.7* RNA probe labels approximately 50% of the basal neurons. In contrast, rare neurons express *M1* and *M9*. β 2-microglobulin (β 2m) is also expressed basally.
(C) PCR amplification of cDNA prepared from a large collection of tissues with primers specific for the *M10* gene family failed to detect any *M10* transcript except in the VNO. Amplification of GAPDH was used as an internal control.

and occludes the A pocket (Burmeister et al., 1994); a leucine at position 167 in H2-M3 similarly fills the A pocket (Wang et al., 1995). The *M1* family, like the *M10* family, has retained the structural characteristics of the classical MHC class I molecules, but, except for W147, none of the key residues typically involved in peptide binding, and mentioned above, have been conserved in all members (Takada et al., 2003). Thus, although we cannot exclude the possibility that *M10s* and *M1s* bind peptides, they would do so in a nonclassical manner.

The *M10* family has other unusual features that distinguish it from classical MHC molecules. The cytoplasmic tails of *M10s* are only two residues long, in contrast to the approximately 30 residue intracellular C terminus found in all class Ia molecules (Shawar et al., 1994). Although class Ib molecules show more divergence in their intra-cellular domain, this is the shortest tail documented for a class Ib molecule. In addition, a 16 bp frameshift eliminates the canonical site of N-linked glycosylation at position 86 of the *M10s*. Instead, the *M10s* have two unusually positioned, potential sites of N-linked glycosylation at residues 198 and 223, the latter

of which, also found in *M1s*, overlaps with the putative CD8 binding motif. Classical MHC molecules signal to a complex of the T cell receptor (TCR) with CD8 and contact the CD8 coreceptor through conserved sequences in the MHC α 3 domain (Maenaka and Jones, 1999). Such glycosylation in vivo could block an interaction of *M10s* and *M1s* with CD8, although there is no indication that CD8 is expressed in the VNO.

The most striking aspect of the *M10* protein sequences is that differences are highly concentrated in the α 1 helix and at the beginning of the α 2 helix (Figures 2A and 2B). The side chains of these residues would point into the peptide binding pocket in MHC class I molecules or upward to interact with TCRs and other protein ligands.

Cellular Logic of *M10* Family Expression

All transcripts of the six presumed functional members of the *M10* family are exclusively expressed in the basal zone of the VNO, where the V2R family of 7 transmembrane receptors is also found (Figure 1B). Do neurons

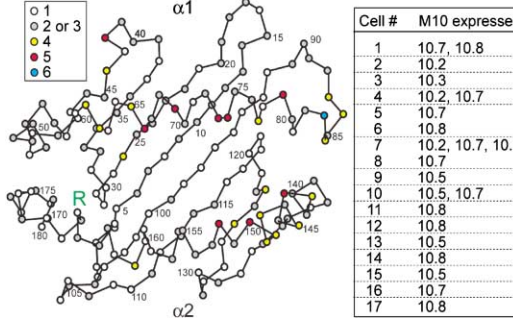
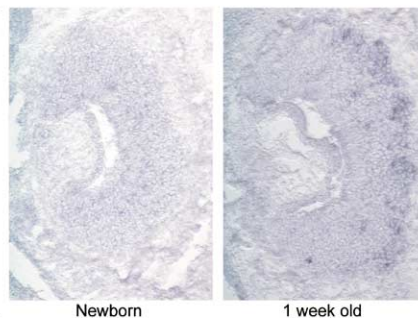
A**B****C**

Figure 2. The M10 Proteins

(A) Alignment of the six M10 protein sequences deduced from isolated cDNAs from strain C57BL/6. Identical residues among M10s are shown in blue; similar residues are shaded in gray. Residues conserved among all MHC class Ia molecules are shown in red for cysteines, orange for tyrosine and tryptophan. Putative sites for N-linked glycosylation are boxed in yellow. The structural domains shared by all class Ia are marked above the sequence and consensus amino acids normally found at the end of the peptide binding groove in MHC class Ia molecules are indicated below the sequences.

(B) Schematic representation of the variability of M10 proteins. The α -carbon backbone of an MHC class I molecule (HLA-A2) is color-coded according to the number of different amino acids found at each position in the sequences of the six M10 proteins. The most variable residues are concentrated in the α_1 helix and the beginning of the α_2 helix.

(C) Single-cell analysis of *M10* expression. RT-PCR on single-cell cDNA from 20 isolated neurons with primers specific for individual *M10* members led to the identification of *M10* transcripts in 17 individual neurons, with most cells expressing only one *M10* gene.

(D) In situ hybridization with *M10* RNA probes on VNO sections demonstrates late onset of expression at one week after birth, while no expression is detected in newborns.

express all or most *M10* genes, or is each *M10* family member expressed by a distinct subset of neurons?

Several independent experiments were performed to address this issue. In situ hybridization on VNO sections shows that each *M10* probe labels approximately half of the cells recognized by all *M10* probes (Figure 1B), suggesting that distinct but largely overlapping subpopulations of *M10*-expressing cells may exist. However, considering that the *M10* family members share high nucleic acid identity, it is unclear to what extent this pattern is due to cross-hybridization between the highly homologous probes.

We therefore designed a second set of experiments

to unambiguously identify specific *M10* transcripts in individual VNO neurons. Sets of primers were designed based on short regions of sequence divergence in the 3'UTR of *M10.2* to *M10.8* cDNAs and were used to preferentially amplify specific *M10* transcripts from G α -positive single-cell cDNAs. Out of 17 *M10*-positive neurons, 13 appeared to express only one *M10* gene (Figure 2C), three neurons expressed two *M10*s, and one cell expressed three *M10*s. In addition, three G α -positive neurons failed to display any *M10* expression, possibly expressing *M10.1*, *M1*, *M7.2*, or *M9*. Interestingly, every cell expressing more than one *M10* also expressed *M10.7*, and among all cells analyzed, *M10.7* and *M10.8*

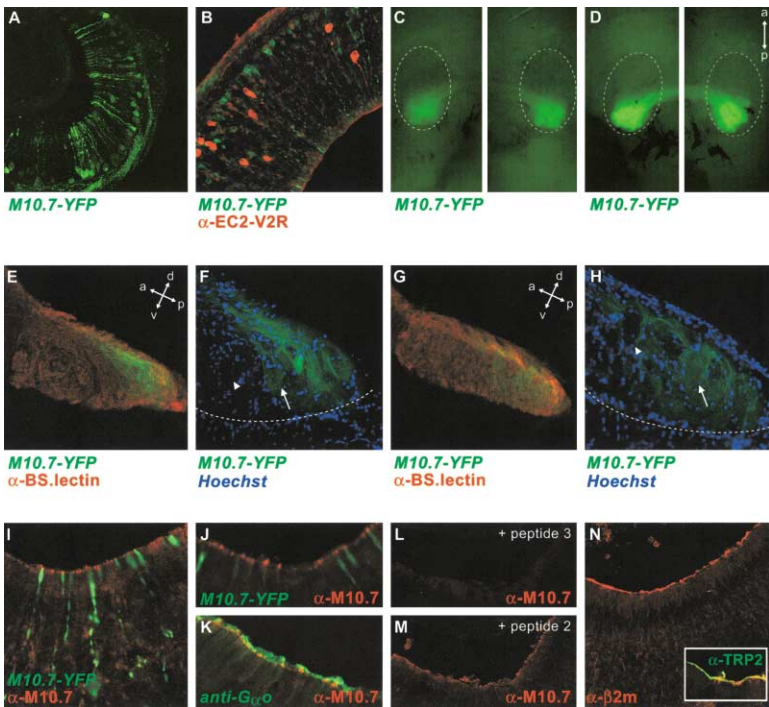


Figure 3. Expression of the *M10.7* Transcripts and the M10.7 Protein in the VNO

(A) Cross-section through the VNO dissected from an *M10.7-ires-tauYFP* mouse shows YFP expression in about 8% of VNO neurons, all located in the most basal half of the neuroepithelium.

(B) Immunostaining with an antibody directed against EC2-V2R on a VNO section from an *M10.7-ires-tauYFP* mouse demonstrates the lack of overlap between EC2-V2R-positive (red) and M10.7-positive cells (green).

(C–H) Projection of M10.7 neurons to discrete loci in the AOB.

(C and D) Whole-mount (dorsal) views of the *M10.7-tauYFP* axons reaching discrete sites of projection in the posterior halves of the right and left AOBs dissected from two different mice.

(E–H) 150 μ m sagittal sections of the *M10.7-tauYFP* AOB.

(E and G) BS lectin coupled to rhodamine (red) preferentially labels the posterior glomerular layer of the AOB and demarcates the boundary between the anterior and posterior domains. M10.7-tauYFP fibers can be seen projecting to discrete glomeruli in the most posterior third of the posterior domain of the AOB.

(F and H) Higher magnification views on sections treated with the Hoechst nuclear stain

identify the discrete glomerular projections of M10.7-expressing neurons (arrows), while other glomeruli do not contain YFP-positive fibers (arrowheads). (a) anterior; (p) posterior; (d) dorsal; and (v) ventral.

(I–N) M10.7, β 2m, $G_{\alpha}o$, and TRP2 are all localized to the VNO dendrite tips, the site of pheromone detection.

(I and J) Immunostaining with the α -M10.7 antibody (red) performed on fixed sections of adult VNO from an *M10.7-ires-tauYFP* mouse line (green) demonstrates protein expression confined to the tip of the green dendrites.

(K) Double immunostaining against M10.7 (red) and $G_{\alpha}o$ (green). M10.7 positive dendrite tips are also $G_{\alpha}o$ -positive and therefore appear yellow; while neighboring $G_{\alpha}o$ -positive, M10.7-negative dendrites appear as green only.

(L and M) Immunostaining of M10.7 dendrites is specifically blocked by peptide 3, against which the anti-M10.7 antibody was raised, but not by peptide 2, corresponding to another region of the M10.7 sequence.

(N) α - β 2m (red) and α -TRP2 (green, inset) immunostainings on sections of rat VNOs clearly show colocalization of these proteins to the dendritic tip where pheromone signal transduction occurs.

appeared relatively more frequently than the other *M10*s (Figure 2C). These results suggest that most, if not all $G_{\alpha}o$ -positive cells express *M10* and that, among *M10*-positive neurons, the majority express only one or few *M10* genes.

Finally, we used a genetic approach to perform a larger scale analysis of the expression of individual *M10* transcripts in the VNO while avoiding the problem of cross-hybridization resulting from the close similarity of the *M10* genes. A transgenic mouse was designed to express the reporter tau-yellow fluorescent protein (YFP) under the control of the *M10.7* gene (see Experimental Procedures). Of six transgenic lines created, four expressed the tau-YFP transgene in an identical pattern, while two showed no expression. An antibody specifically directed against the M10.7 protein (see below) labels the dendritic tips of YFP-positive neurons, confirming correct expression of the transgene in M10.7-expressing cells.

In the VNO of the *M10.7-tauYFP* transgenic mice, YFP is expressed in the cell bodies and dendrites of a small subset of basal neurons (Figure 3A). VNO sections were counterstained with Hoechst nuclear stain in order to quantify the ratio of M10.7-YFP expressing cells. Approximately 8% or 1/12 of the VNO cells express the *M10.7* transgene. Because the basal population repre-

sents only half of the VNO neurons, this result indicates that *M10.7-YFP* is expressed by 16% or 1/6 of the $G_{\alpha}o$ -positive neurons. This figure is compatible with the existence of six largely non-overlapping populations of neurons, each expressing a different *M10* family member.

M10 and V2R Co-Expression

Individual VNO neurons of the basal zone of the neuroepithelium express only one of the estimated 100 to 200 V2R pheromone receptors (Herrada and Dulac, 1997). In turn, the expression of *M10* genes by distinct populations of V2R-positive VNO neurons raises the possibility of a correlation between the expression of a given V2R and a given *M10* in a single cell. Alternatively, *M10*s and V2Rs may be randomly co-expressed. An antibody raised against a synthetic peptide corresponding to a specific sequence motif of the EC2-V2R receptor was used to identify EC2-V2R-expressing neurons in VNO sections from the *M10.7-ires-tauYFP* mice. The EC2-V2R-positive and the M10.7-positive neuronal populations appeared completely segregated, with M10.7 and EC2-V2R never co-expressed in the same cell (Figure 3B). This result argues against a random co-expression of *M10*s and V2Rs and suggests instead that a precise correlation may exist in the expression of both gene families in individual VNO neurons.

This result can be further documented at the level of

the VNO projections to the AOB. Neurons expressing a given V1R or V2R project to discrete glomeruli clustered in large domains of the AOB (Belluscio et al., 1999; Rodriguez et al., 1999; Del Punta et al., 2002a). A precise correlation between the expression of given V2R and M10 genes would likely result in the existence of discrete projection sites of neurons expressing a specific M10. Alternatively, random co-expression of V2Rs and M10s should result in widespread M10.7-positive fiber projections throughout the posterior AOB. Sagittal sections of the AOB from *M10.7-tauYFP* mice, costained with rhodamine-coupled-BS lectin showed that the glomeruli receiving M10.7-positive fibers are invariably positioned in the most posterior third of the posterior AOB (Figures 3C–3H). This pattern is reproducible from animal to animal and the projections in males and females are indistinguishable. In total, the AOBs of 19 animals were examined, representing 9 males and 10 females from 4 transgenic lines. The projection of M10.7-positive axons to a discrete locus within the posterior AOB is consistent with a model in which one M10 is co-expressed with a defined subset of V2Rs.

The direct identification of *M10* transcripts present in neurons expressing a given V2R pheromone receptor confirmed the precise association between V2Rs and M10s. A transgenic mouse line was created in which an ires-tauCFP cassette was placed downstream to the EC1-V2R pheromone receptor gene (E.C. and C.D., unpublished data), such that a population of EC1-V2R-expressing neurons would be labeled with CFP. Nine EC1-V2R-positive, CFP-labeled neurons were picked under the microscope from VNO tissue from these transgenic animals. Remarkably, RT-PCR analysis showed that all 9 EC1-positive single cells express only one unique *M10* member, *M10.5*, while control EC1-negative, CFP-negative cells picked from the same VNO yielded a variety of *M10* transcripts.

Functional Analysis of M10 in the VNO

M10 Expression during Development

Analysis of *M10* expression in the VNO during embryonic and postnatal development showed that *M10* transcripts were first detectable one week after birth (Figure 2D). The numbers of *M10*-expressing cells increased until adulthood, at which stage half of the VNO neurons expressed *M10*. This relatively late onset of expression enabled us to exclude a role for the *M10* family in VNO development and suggested instead a function related to the fully mature sensory organ.

M10 and β2m Proteins Are Localized

in VNO Dendrites

A polyclonal antibody was raised against a synthetic peptide based on a specific sequence of the M10.7 $\alpha 2$ domain. Western blot experiments on VNO protein extracts and on extracts from cells transfected with *M10.7* cDNA resulted in the detection of a band of the predicted size for M10.7 (37 kDa). This band could not be identified in protein samples from other tissues, from cells transfected with other *M10* genes, or from VNO tissue after preincubation of the antibody with the M10.7 peptide against which the antibody was raised (not shown).

Immunostaining of VNO sections from *M10.7-ires-tau-*

YFP mice with the antibody directed against M10.7 showed strict localization of the M10.7 protein in discrete dots lining the VNO lumen, at the very tip of YFP-positive dendrites (Figure 3I), which can be clearly seen on high resolution confocal images (Figure 3J). The specificity of the M10.7 immunostaining was confirmed by lack of signal after preincubation of the α -M10.7 antibody with the antigenic peptide (Figure 3L), and by the absence of immunostaining in M10.7-negative epithelia, such as the VNO respiratory epithelium and the olfactory neuroepithelium. Incubation with an irrelevant peptide leads to the presence of immunostaining (Figure 3M). Immunocytochemistry with various antibodies showed similar protein localization pattern for $\beta 2m$ and the VNO signal transduction components $G\alpha o$ and TRP2 (Figures 3K and 3N). These three proteins appear widely distributed in dendrites along the edge of the VNO lumen, as expected from the expression of the corresponding transcripts in large subsets of VNO neurons. Therefore, it appears that the expression of the $\beta 2m$ and M10.7 proteins is confined to VNO sensory microvilli, where pheromone detection and signal transduction occur.

Molecular Interaction of M10 with β2m and V2Rs

Biochemical analysis enabled us to uncover some of the M10-interacting proteins, providing us with essential clues to the function of M10 molecules in the VNO. Nearly all MHC class I heavy chains form a tight, non-covalent association with $\beta 2m$, which they require for stable display at the cell surface. The co-expression of M10 and $\beta 2m$ in the basal zone of the VNO and colocalization of both proteins in VNO dendrites suggest that they may also associate molecularly. Immunoaffinity chromatography was performed on VNO cell membrane extracts using a resin coupled to an anti- $\beta 2m$ antibody. Western blot analysis of the chromatographic eluate was then performed with antibodies directed against $\beta 2m$, M10.7, TRP2, and with a mix of antibodies specifically directed against V2Rs (Martini et al., 2001) (Figure 4A). Remarkably, in addition to M10.7, V2R proteins could also be detected in the eluate, while TRP2 was absent, suggesting that $\beta 2m$, M10.7, and V2R form a protein complex in the VNO in which TRP2 is absent. Control experiments performed on the spleen failed to detect any of these proteins in the eluate.

The converse experiment was also performed in which antibodies against V2Rs (Martini et al., 2001) were coupled to the resin in order to immunopurify V2R-interacting proteins. The eluate from the column contained M10.7, $\beta 2m$, but not TRP2 (Figure 4B), confirming the specific interaction between M10 molecules, $\beta 2m$, and V2Rs.

A third experiment was performed to further confirm the direct interaction between M10.7, $\beta 2m$, and V2R. A plasmid encoding a soluble fusion protein containing the extracellular domain of M10.7 and the Fc portion of human IgG was used to transfet a mouse spermatogonia cell line propagated in vitro. The choice of this unusual cell line for all our experiments performed in vitro was dictated by the species of origin of the line and by our concern that efficient expression and folding of mouse M10s would require assembly with mouse $\beta 2m$. Control experiments demonstrated absence of V2R and M10 expression in non-transfected cells. The fusion protein was purified from the culture medium, incubated

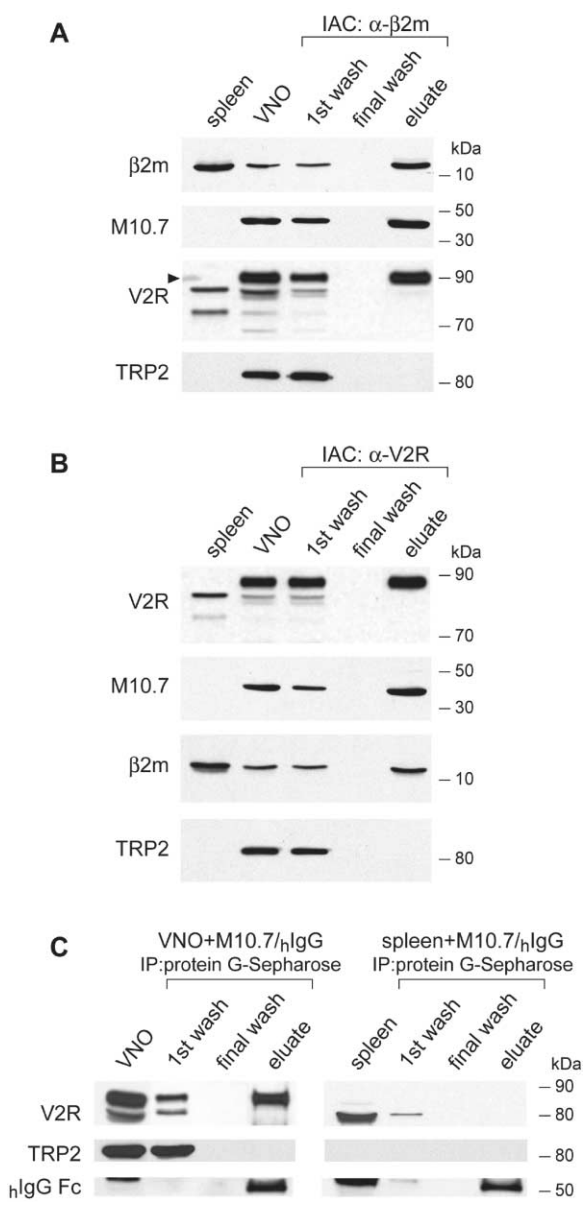


Figure 4. β 2m and M10.7 Form a Multimolecular Complex with V2Rs
(A) Immunopurification of β 2m-interacting proteins from VNO extract. Western blot analysis shows that β 2m (12 kDa), M10.7 (37 kDa), V2R pheromone receptors (90 kDa), and the TRP2 channel (110 kDa) are detected in crude VNO extract (lane 2). In contrast, only β 2m is detected in the spleen (lane 1). Residual amounts of each protein are washed off the Sepharose column (lane 3) and the last wash is clean (lane 4). β 2m, M10.7, and V2Rs are eluted from the beads (lane 5) demonstrating that they are part of a same multimolecular complex in VNO neurons. The TRP2 channel, however, is not found in this complex.

(B) Immunopurification of V2R-interacting proteins from VNO extract. Sepharose column conjugated to α -VN2 and VN4 antibodies was used to immunopurify the V2R-complex from VNO extract. Lanes 1 to 4 are the same as in (A). M10.7 and β 2m are eluted from the beads (lane 5) indicating that they form a multimolecular complex with V2Rs, whereas the TRP2 channel is absent from the complex (lane 5).

(C) In vitro binding experiment showing an interaction between the M10.7-hlgG soluble fusion protein and V2R. Left image: crude VNO extract containing V2R proteins (90 kDa) and TRP2 protein (110 kDa) (lane 1) was incubated with M10.7-hlgG fusion protein and the

with VNO extract, and purified together with interacting proteins on a protein-G-Sepharose column. Western blot analysis confirmed the interaction of M10.7 with β 2m and V2Rs but not TRP2 (Figure 4C, left). No precipitation of V2R was detected when the Fc portion of IgG alone was incubated with the VNO extracts (not shown). A control experiment performed with spleen extract showed the absence of V2Rs and TRP2 (Figure 4C, right) in this tissue.

Thus, we have demonstrated the existence of a VNO-specific multimolecular complex containing M10.7, β 2m, and V2Rs, but not TRP2, suggesting that M10 may act as a coreceptor of the V2R pheromone receptors.

M10 Molecules Participate in the Traffic of V2R to the Cell Surface

Next, we aimed at investigating the functional role of the interaction between M10s and V2Rs. In vitro transfection experiments have shown that V2Rs are unable to localize to the surface of heterologous cells (G. Herrada and C.D., unpublished data), even when prolactin or rhodopsin signal peptides were added to the N terminus of the V2R sequences, tricks which have been instrumental in promoting surface expression of the olfactory and taste receptors in vitro (Krautwurst et al., 1998; Chandashekar et al., 2000). Similarly, native M10s failed to reach the surface of transfected cells in vitro, while control experiments show that transfected class Ia molecules display proper surface expression (not shown). Moreover, initial experiments in which specific V2Rs were separately cotransfected with each M10 member, including with the pair M10.5 and EC1-V2R identified in vivo, consistently resulted in lack of surface expression for both types of molecules.

It has been shown that mouse testicular cells express low levels of β 2m, and other MHC class I-associated molecules such as TAP1, tapasin, and calnexin (Hotta et al., 2000), and that increased expression of β 2m allows surface expression of the MHC class Ib molecule FcRn (Praetor and Hunziker, 2002). We reasoned that, by expressing β 2m along with the M10 molecules, there would be an increase in surface expression for the latter. In fact, cotransfection of M10 with β 2m leads to M10 surface expression (Figure 5D). Based on this result, we designed an experiment in which EC1-V2R and M10.5, known to be co-expressed in vivo, were tagged at their N termini with the rhodopsin signal peptide and myc, respectively, and cotransfected with β 2m in the spermatogonia cell line. Remarkably, in cells cotransfected with EC1-V2R and M10.5, the pheromone receptor and the M10.5 protein colocalize to the plasma membrane, where they could be detected by immunolocalization of the rhodopsin and the myc tags, respectively (Figures 5A–5C).

Thus, the interaction of V2R with M10 appears essential in vitro to provide access of the V2R to the cell surface and suggests a model according to which M10

resulting complex was purified using protein G-Sepharose beads. Residual protein was thoroughly washed from the beads (lanes 1 and 3) and then the complex was eluted (lane 4). The M10.7-hlgG fusion protein forms a complex with V2Rs but not with TRP2. V2R and TRP2 are not detected in the spleen (right image).

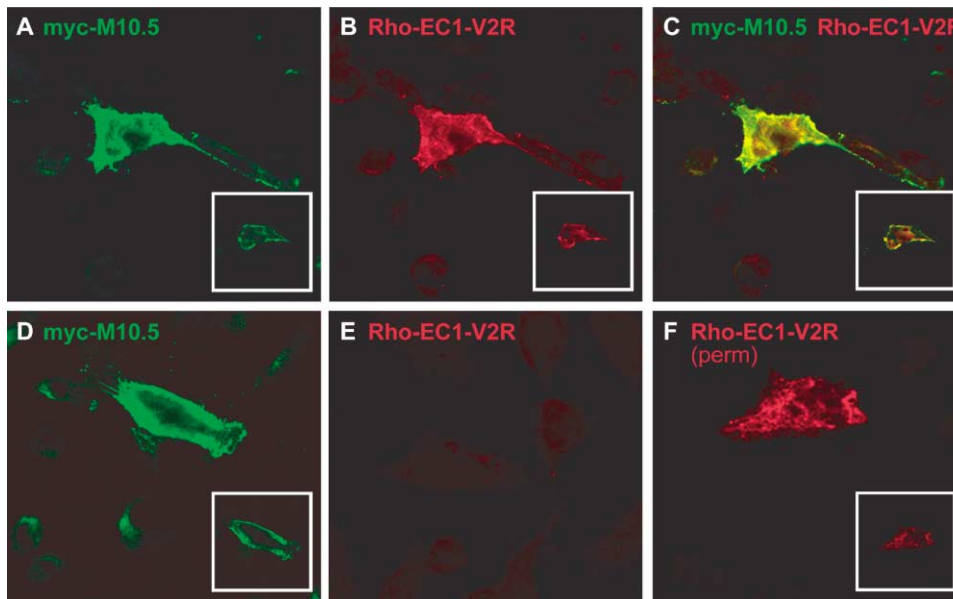


Figure 5. M10.5 in the Presence of β 2m Promotes the Traffic of EC1-V2R Receptor to the Plasma Membrane

(A–C) Spermatogonia cells propagated in vitro were cotransfected with DNA constructs coding for the EC1-V2R pheromone receptor, mouse β 2m, and the M10.5 protein. Proteins were visualized by immunostaining to detect myc (M10.5) and rhodopsin (EC1-V2R) tags, labeled in green (A), and red (B), respectively. Cotransfected cells exhibit colocalization of both proteins at the cell surface (C) in non-permeabilized preparations.

(D) The M10.5 protein is detected at the cell membrane (green) in spermatogonia cells cotransfected with myc-M10.5 and β 2m in the absence of EC1-V2R.

(E and F) Spermatogonia cells transfected with the EC1-V2R receptor alone indicate absence of membrane immunostaining (E) and intracellular retention (F, permeabilized cells) of the rhodopsin-tagged protein (Rho-EC1, red).

Confocal images in parts (A–E) are thick optical sections to show staining in the whole plasma membrane of the transfected cell. Insets (A–D) correspond to thin optical sections of the same cell to evidence cell surface staining.

molecules escort the V2R pheromone receptors during traffic to the cell surface.

Molecular and Behavioral Analysis of the β 2m^{−/−} Mutant

Our in vitro experiments suggest that β 2m and M10s play an essential role in escorting V2R molecules to the cell surface. The availability of a β 2m^{−/−} mutant line enabled us to directly assess this hypothesis in vivo. In a first set of experiments, we aimed at visualizing the proper localization of V2Rs to sensory terminals. An antibody directed against a peptide based on the sequence of the cytoplasmic domain of the EC2-V2R pheromone receptor strongly recognized the cell body and proximal portion of the sensory dendrite in subsets of VNO neurons, but failed to label the dendritic tips, perhaps by lack of accessibility of the corresponding epitope. In contrast, the anti-VN4/V2R antiserum, raised against the extracellular domain of the rat VN4/V2R protein (Martini et al., 2001) generated distinct immunostaining of the cell body, dendrites, and sensory terminals of subsets of VNO neurons. Therefore, we were able to use this antiserum to assess the localization of mouse V2R recognized by the reagent to the tip of VNO sensory dendrites in both wild-type and β 2m^{−/−} mice. Strikingly, the labeling of the VN4/V2R-positive dendritic terminals was consistently absent in the β 2m^{−/−} mouse, suggesting a defect of receptor transport to that site (Figures 6C–6D). Control immunostaining with other members of the transduction apparatus, such as TRP2

and G α O, (Figures 6A and 6B) showed no difference between controls and β 2m^{−/−} mice.

A defect in pheromone receptor localization to sensory terminals is likely to impair the pheromone sensory response in the corresponding neurons. We therefore performed behavioral analysis of control and β 2m^{−/−} adult males as previously described (Stowers et al., 2002). Repeated trials of β 2m^{−/−} adult males in the resident/intruder test ($n = 20$) demonstrated a consistent lack of aggressive behavior of the mutant toward castrated males swabbed with male pheromones, in contrast to the behavior of control animals ($n = 6$) (Figure 6E). Moreover, in contrast to TRP2^{−/−}, in which the entire VNO function is genetically ablated, β 2m^{−/−} adult males appear able to discriminate the sex of conspecifics and do not attempt to mate with other males (not shown). Because β 2m is widely expressed in the brain and in other tissues, one cannot ascertain the exact origin of the observed phenotype without additional experiments such as the specific rescue of β 2m expression in the VNO. Nevertheless, our behavioral data are consistent with a partial defect in the pheromone sensory response, such as that generated by lack of proper V2R function.

Discussion

We have reported here the molecular, cellular, and functional characterization of the M10 family of MHC class Ib genes. A first striking feature of the *M10* genes is their exclusive expression in the VNO. Interestingly *M10*

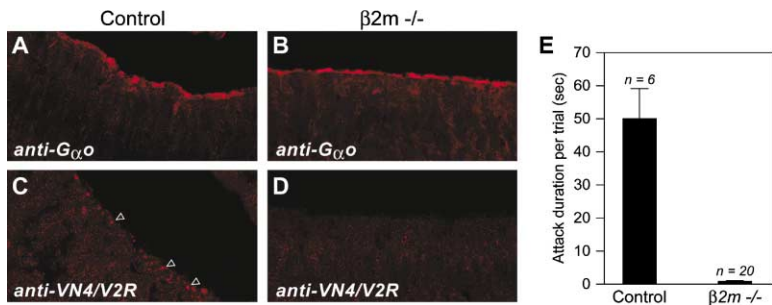


Figure 6. Molecular and Behavioral Analysis of the $\beta 2m^{-/-}$ Mouse Line

(A–D) Immunostaining of VNO sections dissected from adult wild-type (A and C) and $\beta 2m^{-/-}$ (B and D) mice. While $G\alpha o$ expression appear indistinguishable in VNO from wild-type (A) and $\beta 2m^{-/-}$ mutant (B), localization of the VN4/V2R pheromone receptor to the dendritic tip along the lumen of the VNO, is evident in the wild-type (arrowheads in C), but appears severely compromised in the $\beta 2m^{-/-}$ mutant line (D).

(E) Adult males of the $\beta 2m^{-/-}$ mouse line do not display male-male aggression in the resident/intruder behavioral assay. Quantification of resident average attack durations in a 10 min trial against castrated male intruders swabbed with male urine demonstrates the lack of aggression of the $\beta 2m^{-/-}$ adult males compared to control animals.

homologs appear absent from the genome of the fugu fish (*Takifugu rubripes*) despite the presence of genuine V2Rs, suggesting that the function of M10s is a more recent evolutionary acquisition than the emergence of the V2R family in pheromone detection. Moreover, within the VNO, members of the *M10* family appear restricted to specific subsets of V2R-positive neurons of the basal VNO neuroepithelium, such that individual neurons express only one or a few *M10* genes. The expression of a given *M10* by a restricted set of chemosensory neurons, in a manner quite reminiscent to the choice of olfactory and pheromone receptors (Buck and Axel, 1991; Dulac and Axel, 1995), appears extremely unusual for MHC class I genes. Class Ia MHC molecules are expressed in association with $\beta 2m$ at the surface of most cells and play an important role in the immune system by signaling the presence of foreign invaders to CD8-positive cytotoxic T lymphocytes (CTLs) (Maenaka and Jones, 1999). Originally thought to be absent in the brain, the wide and dynamic expression of class Ia and Ib molecules during neural development and by neurons undergoing activity-dependent modifications has led to the proposal that they additionally play a role in synaptic development and plasticity (Corriveau et al., 1998; Huh et al., 2000). The absence of M10 expression during key steps of vomeronasal development such as the onset of receptor expression and axon guidance to specific targets in the AOB, together with the strict localization of the M10 molecules to the tip of sensory dendrites and their absence from synaptic terminals exclude the possibility that M10s may play a similar developmental or synaptic role. Olfactory and V1R receptors have been shown to participate to the process of sensory axon guidance to appropriate glomeruli (Wang et al., 1998; Belluscio et al., 1999; Rodriguez et al., 1999). Our data suggest that, if V2R were to play a similar role in axon pathfinding, they would require a mode of activity that is independent of M10 expression. The expression of M10s at the tip of VNO dendrites suggests instead a role in the fully mature VNO, likely in the process of pheromone detection. It has been shown that mice prefer to mate with conspecifics of a dissimilar MHC group, and that the MHC-based mating preference involves chemosensory recognition (Penn and Potts, 1998). The expression of MHC class Ib molecules in the VNO opens attractive possibilities of modulating the pheromone-evoked response, for example, by coincident detection of pheromone ligands and of small molecules associ-

ated with the MHC group of a conspecific. However, the M10s and M1s display minimal polymorphism between haplotypes (Takada et al., 2003; E.P.J., unpublished data) and might therefore not be able to form the structural basis of an *H2*-linked discrimination.

The nonclassical MHC class Ib molecules, which share sequence and structural homology with class Ia molecules, but tend to display lower polymorphism and a more restricted expression profile, have been shown to participate in various immune and non-immune functions (Shawar et al., 1994). Moreover, some MHC class Ib proteins engage in highly specific molecular interactions that may resemble the binding of M10s to V2Rs. FcRn binds and transfers ingested maternal IgG across the intestine of neonatal rodents, while the hereditary hemochromatosis protein (HFE) regulates iron absorption by binding to the transferrin receptor. Although FcRn and HFE display a structure similar to the standard MHC fold, they do, however, lack many conserved residues known in class Ia proteins to interact with peptides. Moreover, instead of a tryptophan in position 167 of the equivalent class I sequence, they have an arginine or a glutamine, respectively, that occlude the end of the groove, making it non-functional. Interestingly, sequence analysis of M10s shows very similar characteristics, with only subsets of the key residues typically involved in peptide binding still present, and a potentially obstructing arginine in position 167. In addition, the VNO does not express TAP1 and TAP2, molecules which are essential for loading the peptide into the groove of MHC class Ia molecules. Thus, although we cannot exclude that M10s have retained a functional groove involved in the binding of a peptide or other small ligands, they would bind such molecules in a nonclassical manner.

Our data demonstrate the existence of specific multimolecular complexes composed of M10s, V2Rs, and $\beta 2m$ and confined to VNO dendrites, the site of pheromone detection and signal transduction. Furthermore, we have provided evidence supporting a cellular and molecular specificity in the M10-V2R interaction, such that a given *M10* gene is transcribed in neurons expressing a defined subset of V2Rs, leading to the exclusive interaction between a given V2R and a specific M10. This selective cellular and molecular association generates molecularly distinct compartments in the VNO and in the AOB, each specified by the expression of a given M10 and a selected subset of V2Rs. The existence of common features among the V2Rs of a given subset,

and the possible functional significance of these compartments will require further investigations. Interestingly, the behavioral phenotype of the $\beta 2m^{-/-}$ mouse line, in which only V2R-related behavior detection is likely to be affected in the pheromone sensory response, may provide an indication of distinctive roles played by the apical and basal neuronal compartments of the VNO. We have shown that the $\beta 2m^{-/-}$ mouse line does not display male-male aggression, as previously described in the TRP2 $^{-/-}$ mouse line (Stowers et al., 2002). However, in contrast to the behavior of TRP2 $^{-/-}$ males in which the entire VNO sensory detection is impaired, $\beta 2m^{-/-}$ males, which are likely to retain fully functional V1R-related pheromone detection, do not display sexual attempts toward other males, suggesting normal sex discrimination. Thus, the V1R- and the V2R-positive VNO neuronal populations may play distinct roles in controlling sex discrimination and pheromone-induced aggression, respectively.

How is the M10-V2R interaction achieved? In FcRn, binding to the IgG occurs on the side of the $\alpha 1\alpha 2$ domains (Burmeister et al., 1994; Wilson and Bjorkman, 1998). As in the MHC-TCR recognition, the interaction between HFE and the transferrin receptor involves the $\alpha 1$ and $\alpha 2$ domain helices, but the details of the interaction are substantially different, occurring in *cis* between adjacent membrane proteins, and involving most of the $\alpha 1$ helix and only the extremity of the $\alpha 2$ helix (Bennett et al., 2000). Remarkably, the same regions are the most divergent among M10 sequences (see Figure 2B), opening the possibility that a similar mechanism may occur in the recognition between a given M10 and a subset of V2Rs. Indeed, the considerable variation in the V2R extracellular domain sequences (Herrada and Dulac, 1997; Matsunami and Buck, 1997; Ryba and Tirindelli, 1997) may permit both the pheromone ligand recognition and the interaction with a given M10. Alternatively, the M10-V2R interaction may involve conserved regions in each protein family, and the variable motifs in V2R and M10 families may be devoted to the specific recognition of small ligands.

What is the role of the V2R-M10 interaction? It has been recently demonstrated that a growing number of GPCRs such as the GABA_B receptors (Margeta-Mitrovic et al., 2000), the T1R taste receptors (Li et al., 2002; Nelson et al., 2002), and the calcitonin receptor (McLatchie et al., 1998) engage in the formation of heteromers. Remarkably, the interaction of GPCRs with accessory molecules induces profound modifications in the receptor-ligand binding specificity. Moreover, structural analysis of the HFE-transferrin receptor interaction (Bennett et al., 2000) revealed the existence of important conformational changes in the structure of the transferrin receptor resulting from the binding to its MHC class I-like partner. Similarly, V2R function is likely to be significantly modified by the interaction with M10s in at least one of two ways. Firstly, our *in vitro* and *in vivo* data suggest that the specific association between M10 and V2R is required for proper escort of the pheromone receptor to the cell surface and the sensory terminals, a function that may involve providing necessary subcellular targeting signals or modifying the conformation of the receptor to ensure proper transport and stability of a given V2R at the dendritic tip. In addition, and

perhaps more importantly, the molecular association between M10 and V2R at the surface of VNO dendrites is likely to significantly alter the mechanism and potentially specificity of pheromone recognition, thus adding a novel and unexpected layer of complexity to the process of pheromone detection.

Experimental Procedures

Single-Cell cDNA Library Screening

Single cells were picked from dissociated VNOs of adult Lewis rats (Dulac and Axel, 1995). cDNA synthesis and amplification, and cDNA library packaging were performed as previously described (Dulac and Axel, 1995). To screen for markers of the apical ($G_{\alpha 12}$) zone of the VNO, a $G_{\alpha 12}$ cell cDNA library was differentially screened with two sets of ^{32}P -labeled cDNA probes: regular $G_{\alpha 10}$ cell cDNA or $G_{\alpha 12}$ cell cDNA enriched for $G_{\alpha 12}$ -specific genes according to the "cDNA Difference Analysis" protocol (Hubank and Schatz, 1994). Clones unique to the $G_{\alpha 12}$ cell were selected. Similar protocol led to the identification of clones unique to $G_{\alpha 10}$ cells.

Mouse M10 homologs were isolated by screening a C57BL/6J VNO cDNA library using the clone 144 and mouse M10.7 cDNA clone as probes. Sequences were aligned using MacVector and ClustalX softwares (Oxford Molecular Group). Primers J68 (5'-cga aca cat gtg acc ca-3') and J69 (5'-caa gaa cca ggc cga tga-3'), were used to amplify all six expressed M10 family members.

In Situ Hybridization

Anti-sense RNA probes were synthesized from full-length cDNA templates for M10, $\beta 2m$, TAP-1 or -2 genes, and hybridization was performed as described (Schaeren-Wiemers and Gerfin-Moser, 1993). Images were captured on a Leitz DMRB microscope (Leica) coupled to a ProgRes3012 digital camera (Kontron Electronic).

Generation of M10.7-tauYFP and EC1-V2R-tauCFP Transgenic Mice

The ires-tauYFP cassette was created by replacing the lacZ sequence with yellow fluorescent protein (YFP) in the IRES-taulacZ cassette (from Belluscio et al., 1999). This cassette was inserted into a PacI site created 3 codons after the M10.7 stop codon in a shuttle vector (Yang et al., 1997) containing 3 kb of mouse genomic DNA centered around the termination codon of the M10.7 sequence. Homologous recombination between the shuttle vector and BAC ctb553n23, containing the M10.7 locus, yielded a modified BAC containing the M10.7-ires-tauYFP transgene, which was in turn microinjected into pronuclei of B6/CBA F1 oocytes.

Similar strategy led to the construction of an IRES-tauCFP cassette, which was inserted 3 bases downstream of the EC1-V2R gene in a shuttle vector containing 1 kb of genomic DNA centered around the EC1-V2R stop codon. Homologous recombination between the shuttle vector and BAC RPCI-22 488 H14 yielded a modified BAC containing the EC1-IRES-tauCFP transgene.

Single-Cell PCR Analysis

cDNA from a series of single VNO neurons picked from adult C57BL/6 mice was prepared as described above. Individual M10 genes were amplified from these cDNA samples using specific pairs of primers and annealing temperatures: M10.2 (J82/85, 55°C); M10.3 (J82/83, 55°C); M10.5 (J86/88, 50°C); M10.7 (J82/84, 60°C); and M10.8 (J87/88, 50°C). Oligonucleotides were: J82: 5'-gaa ctg tgg tga tt ttc tgg-3'; J83: 5'- ctc ttg tta aac atg gaa-3'; J84: 5'-ctc ttg tta aac ttg gag-3'; J85: 5'-tca tgt taa aga tga cag-3'; J86: 5'-taa gta caa cat gag a-3'; J87: 5'-taa aga caa cac aag g-3'; and J88: 5'-cta ata ttg aag gag gaa-3'.

In other set of experiments, VNOs from EC1-V2R-tauCFP transgenic mice were dissected and embedded in 3% agarose. Vibratome 250 μ m sections were taken and visualized on a Leica DMLFS microscope. Single EC1-CFP-expressing neurons were isolated under a Hamamatsu C2400 infrared camera by suction into a microcapillary needle and seeded into a PCR tube.

Antibodies and Immunostaining

An eight-residue peptide [EYV/KSRWD] based on the sequence of M10.7 was synthesized and used to produce IgY polyclonal antiserum (AvesLab). Chicken antiserum was also raised against the EC2-V2R pheromone receptor (G. Herrada and C.D., unpublished data). Polyclonal rabbit antisera raised against VN2 and VN4 V2Rs from rat (Martini et al., 2001), polyclonal rabbit antiserum against the TRP2 channel (Liman et al., 1999), and mouse monoclonal antibody against rat β 2m (SEROTEC) were also used.

Immunostaining on VNOs from adult C57BL/6J (The Jackson Laboratory) or M10.7-*tau*YFP mice was performed as before (Liman et al., 1999), except that an extra step of postsectioning fixation with 100% acetone at -20°C for 10 min was added before blocking with 10% BlockHen (Aves lab). Antibodies were used at the following dilutions: α -M10.7 (1:1000), α - β 2m (1:500), α -TRP2 (1:1000), α -G α o (1:200), Cy2- or Cy3-conjugated secondary antibodies (1:500; Jackson ImmunoResearch Labs).

Vibratome sections (150 μ m) of M10.7-*tau*YFP AOBs were incubated for 2 hr at room temperature with rhodamine-conjugated *Ban-deiraea simplicifolia* Lectin I (BS lectin, 1:500; Vector Laboratories) in TNT/0.5% Triton X-100/2% fetal bovine serum.

Images were captured on an LSM510 confocal microscope (Zeiss). Whole-mount images of AOBs were obtained with an MZFLIII stereomicroscope coupled to a Leica DC500 digital camera.

Immunoaffinity Chromatography and In Vitro

Protein Interaction

VNOs from 40 female C57BL/6 mice, 4–8 weeks of age (The Jackson Laboratory), were homogenized in lysis buffer (10 mM Tris-HCl, [pH 7.5]; 150 mM NaCl; 5 mM iodoacetamide; 1 mM PMSF; proteinase inhibitor mix [aprotinin, pepstatin, leupeptin]) at 4°C. Cell membrane extract was obtained by pelleting at 55,000 rpm followed by resuspension in lysis buffer containing 0.5% NP-40. Rabbit α -human β 2m antibody (DAKO Corp.) was bound to activated Sepharose using the Seize Primary Mammalian Immunoprecipitation Kit (Pierce). The coupled resin was incubated with the cell membrane extract overnight at 4°C. Washes and elution were performed according to the Pierce kit specifications. Aliquots of eluates and washes (20 μ l), and spleen and VNO samples (15 μ g total protein) were subjected to Western blot analysis, as described before (Stowers et al., 2002). Primary antibodies were a mixture of anti-VN2 and anti-VN4 antisera (1:1000 each), anti-M10.7 antiserum (1:200), anti-TRP2 (1:1000) and anti-mouse β 2m (1:100). All secondary antibodies were horseradish peroxidase-conjugated (Jackson ImmunoResearch Laboratories). In the V2R affinity chromatography experiment, the resin was coupled to an equimolar mixture of anti-VN2 and anti-VN4 antibodies (Martini et al., 2001).

The extracellular part of M10.7 (leader peptide and α 1, α 2, and α 3 domains) was amplified from the M10.7 cDNA using primers FP1 (5'-atc atc gga tcc cca tt cag ctt gag agg ct-3') and FP2 (5'-atc atc aag ctt acc atg agg aac cct-3') and cloned into HindIII/BamHI sites of plasmid pS521 (Houimel et al., 2001) to generate a fusion between M10.7 and the Fc portion of human IgG. This construct was transiently transfected into SV40-transformed mouse spermatogonia cells (GC-1 spg; ATCC) using the Lipofectamine 2000 reagent (Invitrogen). The fusion protein was purified from the supernatant of transfected cells on a protein G-Sepharose column and concentrated on Centricon microconcentrators (Millipore). VNO or spleen membrane extracts were incubated overnight at 4°C with 400 μ g of fusion protein before addition, for 2 hr at 4°C, of 50 μ l of 50% protein G-Sepharose slurry (Amersham) pre-equilibrated with PBS. Protein complexes were eluted in 50 μ l of 2× SDS electrophoresis loading buffer. Crude spleen and VNO samples, eluate, and washes were resolved on a 9.5% polyacrylamide SDS-PAGE gel and subjected to Western blot analysis using either a mixture of anti-VN2 and VN4 antibodies, anti-TRP2 antibody, or simply peroxidase-conjugated anti-human secondary antibody (1:1000).

Cotransfection Experiments in Mammalian Cultured Cells

Mouse β 2m cDNA was amplified by PCR using primers FA1 (5'-atg atg cca tgg ctc gct cgg tga cc-3') and FP135 (5'-atc atc tct aga ttg cta tt tct tct gcg tgc-3'), which insert Ncol and XbaI at the 5' and 3' ends of the cDNA, respectively. This Ncol/XbaI fragment was

subcloned into the IRES-taulacZ cassette to replace the taulacZ sequence, creating an IRES- β 2m cassette. EC1-V2R was amplified from its cDNA clone using primers EC1RhoF (5'-atg ctg ctc tct tgg ctt ctt atc g-3') and EC1RhoR (5'-cta tgt tt aag aaa agt ttg ccc-3') and cloned into Ncol/Nhel sites of the pEAK10 plasmid and subcloned into NotI/HindIII sites of pCDNA3.1zeo to generate a construct coding for EC1-V2R with a rhodopsin tag (Rho) at the N terminus (Rho-EC1-V2R). The IRES- β 2m cassette was then inserted after the stop codon of Rho-EC1-V2R to generate a Rho-EC1-V2R-IRES- β 2m construct.

The M10.5 cDNA sequence (α 1, α 2, α 3, and transmembrane domains) was amplified from the M10.5 cDNA using primers FP143 (5'-gag gat ctg cac tgg ctg aag act ttc agg-3') and FP2001 (5'-cat ctc tag att att tcc tcc aca cca gaa aaa tc-3'). The leader peptide was separately amplified using primers FP2 and FP155 (5'-cag cca gtg cag atc ctc ttc-3'). The two PCR fragments were combined and fused together by PCR using primers FP2 and FP2001, generating a fragment containing M10.5 with a myc tag between the leader peptide and the α 1 domain.

Constructs coding for Rho-EC1-V2R-IRES- β 2m and myc-tagged M10.5 were transiently transfected individually or in combination into cultured spermatogonia cells using the Lipofectamine 2000 reagent. M10.5 was also cotransfected with a construct containing the mouse β 2m cDNA in pCDNA3.1 in the absence of Rho-EC1-V2R. One day after transfection, cells growing on Lab-Tek II chambered glass slides (NUNC) were fixed with 4% paraformaldehyde and subjected to immunostaining. In some cases, cells were permeabilized for 1 min with 0.1% Triton X-100 in 1× PBS before blocking. Antibodies used were: rabbit polyclonal anti-myc antibody (1:200; Santa Cruz Biotechnology) and mouse monoclonal anti-rhodopsin tag antiserum (1:500). Secondary antibodies were Cy2-conjugated anti-rabbit and Cy3-conjugated anti-mouse antibodies (Jackson ImmunoResearch Laboratories).

Behavioral Analysis

Territorial aggression and mating assays were performed and analyzed exactly as described in earlier publication (Stowers et al., 2002). Trials were performed on adult β 2m^{-/-} male mice (n = 8, 20 trials) obtained from The Jackson Laboratory, and on control TRP2^{+/+} (n = 3, 6 trials) to maximize the matching of genetic backgrounds.

Acknowledgments

We wish to acknowledge Renate Hellmiss-Peralta for artistic work and illustrations and Cecilia Lee for help with the manuscript. We thank Jolanta Dubauskaite for mouse transgenic work; Gilles Herrada, Shlomo Wagner, and Lorena Pont-Lezica for providing unpublished reagents and useful advice; M.E. Klein, Qiarong Jiang, and Enxi Chu for technical assistance; and Drs. Jack Strominger, Richard Axel, and Carla Schatz for helpful discussions. Plasmid pS521 was kindly provided by Dr. P. Schneider. Anti-VN2 and anti-VN4 rabbit antisera were obtained from Dr. Roberto Tirindelli and anti-rhodopsin from Drs. Randy Reed, Jeremy Nathans, and Paul Hargrave. This work was supported by the Howard Hughes Medical Institute, and by grants 3903-01 of NIH-NIDCD (C.D.) and AI37818 of NIH (K.F.L.).

Received: January 6, 2003

Revised: February 13, 2003

References

- Arepalli, S.R., Jones, E.P., Howcroft, T.K., Carlo, I., Wang, C.R., Lindahl, K.F., Singer, D.S., and Rudikoff, S. (1998). Characterization of two class I genes from the H2-M region: evidence for a new subfamily. *Immunogenetics* 47, 264–271.
- Belluscio, L., Koentges, G., Axel, R., and Dulac, C. (1999). A map of pheromone receptor activation in the mammalian brain. *Cell* 97, 209–220.
- Bennett, M.J., Lebron, J.A., and Bjorkman, P.J. (2000). Crystal structure of the hereditary haemochromatosis protein HFE complexed with transferring receptor. *Nature* 40, 46–53.
- Buck, L., and Axel, R. (1991). A novel multigene family may encode

- odorant receptors: a molecular basis for odor recognition. *Cell* 65, 175–187.
- Burmeister, W.P., Gustin, L.N., Simister, N.E., Blum, M.L., and Bjorkman, P.J. (1994). Crystal structure at 2.2 Å resolution of the MHC-related neonatal Fc receptor. *Nature* 372, 336–343.
- Chandrashekhar, J., Mueller, K.L., Hoon, M.A., Adler, E., Feng, L., Guo, W., Zuker, C.S., and Ryba, N.J.P. (2000). T2Rs function as bitter taste receptors. *Cell* 100, 703–711.
- Corriveau, R.A., Huh, G.S., and Shatz, C.J. (1998). Regulation of class I MHC gene expression in the developing and mature CNS by neural activity. *Neuron* 21, 505–520.
- Del Punta, K., Puche, A., Adams, N.C., Rodriguez, I., and Mombaerts, P. (2002a). A divergent pattern of sensory axonal projections is rendered convergent by second-order neurons in the accessory olfactory bulb. *Neuron* 35, 1057–1066.
- Del Punta, K., Leinders-Zufall, T., Rodriguez, I., Jukan, D., Wysocki, C., Ogawa, S., Zufall, F., and Mombaerts, P. (2002b). Deficient pheromone responses in mice lacking a cluster of vomeronasal receptor genes. *Nature* 419, 70–74.
- Dulac, C. (2000). Sensory coding of pheromone signals in mammals. *Curr. Opin. Neurobiol.* 10, 511–518.
- Dulac, C., and Axel, R. (1995). A novel family of genes encoding putative pheromone receptors in mammals. *Cell* 83, 195–206.
- Halpern, M., Jia, C., and Shapiro, L.S. (1998). Segregated pathways in the vomeronasal system. *Microsc. Res. Tech.* 41, 519–529.
- Herrada, G., and Dulac, C. (1997). A novel family of putative pheromone receptors on mammals with a topographically organized and sexually dimorphic distribution. *Cell* 90, 763–773.
- Hotta, C., Nagata, T., Nakazawa, M., Fujimaki, H., Yoshinari, M., and Minami, M. (2000). Impaired expression of MHC class I molecules on mouse esticular germ cells is mainly caused by the post-transcriptional mechanism. *Immunogenetics* 51, 624–631.
- Houimel, M., Schneider, P., Terskikh, A., and Mach, J.P. (2001). Selection of peptides and synthesis of pentameric peptobody molecules reacting specifically with ErbB-2 receptor. *Int. J. Cancer* 92, 748–755.
- Hubank, M., and Schatz, D.G. (1994). Identifying the differences in mRNA expression by representation difference analysis of cDNA. *Nucleic Acids Res.* 22, 5640–5648.
- Huh, G.S., Boulanger, L.M., Du, H., Riquelme, P.A., Brotz, T.M., and Shatz, C.J. (2000). Functional requirement for class I MHC in CNS development and plasticity. *Science* 290, 2155–2159.
- Jones, E.P., Kumanovics, A., Yoshino, M., and Fischer-Lindahl, K. (1999). Mhc class I and non-class I gene organization in the proximal H2-M region of the mouse. *Immunogenetics* 49, 183–195.
- Krautwurst, D., Yau, K.W., and Reed, R.R. (1998). Identification of ligands for olfactory receptors by functional expression of a receptor library. *Cell* 95, 917–926.
- Kumánovics, A., Takada, T., and Fischer Lindahl, K. (2003). Genomic organization of the mammalian MHC. *Annu. Rev. Immunol.* 21, 629–657.
- Leybold, B.G., Yu, C.R., Leinders-Zufall, T., Kim, M.M., Zufall, F., and Axel, R. (2002). Altered sexual and social behaviors in trp2 mutant mice. *Proc. Natl. Acad. Sci. USA* 99, 6376–6381.
- Li, X., Staszewski, L., Xu, H., Durick, K., Zoller, M., and Adler, E. (2002). Human receptors for sweet and umami taste. *Proc. Natl. Acad. Sci. USA* 99, 4692–4696.
- Liman, E.R., Corey, D.P., and Dulac, C.D. (1999). TRP2: A candidate transduction channel for mammalian pheromone sensory signaling. *Proc. Natl. Acad. Sci. USA* 96, 5791–5796.
- Maenaka, K., and Jones, E.Y. (1999). MHC superfamily structure and the immune system. *Curr. Opin. Struct. Biol.* 9, 745–753.
- Margeta-Mitrovic, M., Jan, Y.N., and Jan, L.Y. (2000). A trafficking checkpoint controls GABA(B) receptor heterodimerization. *Neuron* 27, 97–106.
- Martini, S., Silvotti, L., Shiraz, A., Ryba, N.J.P., and Tirindelli, R. (2001). Co-expression of putative pheromone receptors in the sensory neurons of the vomeronasal organ. *J. Neurosci.* 21, 843–848.
- Matsunami, H., and Buck, L.B. (1997). A multigene family encoding a diverse array of putative pheromone receptors in mammals. *Cell* 90, 775–784.
- McLatchie, L.M., Fraser, N.J., Main, M.J., Wise, A., Brown, J., Thompson, N., Solari, R., Lee, M.G., and Foord, S.M. (1998). RAMPs regulate the transport and ligand specificity of the calcitonin-receptor-like receptor. *Nature* 393, 333–339.
- Nelson, G., Chandrashekhar, J., Hoon, M.A., Feng, L., Zhao, G., Ryba, N.J., and Zuker, C.S. (2002). An amino-acid taste receptor. *Nature* 416, 199–202.
- Penn, D., and Potts, W. (1998). How do major histocompatibility complex genes influence odor and mating preferences? *Adv. Immunol.* 69, 411–436.
- Praetor, A., and Hunziker, W. (2002). B2-microglobulin is important for cell surface expression and pH-dependent IgG binding of human FcRn. *J. Cell Sci.* 115, 2389–2397.
- Rodriguez, I., Feinstein, P., and Mombaerts, P. (1999). Variable patterns of axonal projections of sensory neurons in the mouse vomeronasal system. *Cell* 97, 199–208.
- Ryba, N.J.P., and Tirindelli, R. (1997). A new multigene family of putative pheromone receptors. *Neuron* 19, 371–379.
- Schaeren-Wiemers, N., and Gerfin-Moser, A. (1993). A single protocol to detect transcripts of various types and expression levels in neural tissue and cell cultures: in situ hybridization using digoxigenin-labeled cRNA probes. *Histochemistry* 100, 431–440.
- Shawar, S., Vyas, J.M., Rodgers, J.R., and Rich, R.R. (1994). Antigen presentations by major histocompatibility complex class I-B molecules. *Annu. Rev. Immunol.* 12, 839–880.
- Sorensen, P.W., Christensen, T.A., and Stacey, N.E. (1998). Discrimination of pheromonal cues in fish: emerging parallels with insects. *Curr. Opin. Neurobiol.* 8, 458–467.
- Stowers, L., Holy, T.E., Meister, M., Dulac, C., and Koentges, G. (2002). Loss of sex discrimination and male-male aggression in mice deficient for TRP2. *Science* 259, 1493–1500.
- Takada, T., Kumanovics, A., Amadou, C., Yoshino, M., Jones, E., Athanasiou, M., Evans, G., and Fischer Lindahl, K. (2003). Species-specific class I gene expansions formed the telomeric 1 Mb of the mouse major histocompatibility complex. *Genome Res.*, in press.
- Wang, C.R., Castano, A.R., Peterson, P.A., Slaughter, C., Lindahl, K.F., and Deisenhofer, J. (1995). Nonclassical binding of formylated peptide in crystal structure of the MHC class Ib molecule H2-M3. *Cell* 82, 655–664.
- Wang, F., Nemes, A., Mendelsohn, M., and Axel, R. (1998). Odorant receptors govern the formation of a precise topographic map. *Cell* 93, 47–60.
- Wilson, I.A., and Bjorkman, P.J. (1998). Unusual MHC-like molecules: CD1, Fc receptor, the hemochromatosis gene product and viral homologs. *Curr. Opin. Immunol.* 10, 67–73.
- Yang, X.W., Model, P., and Heintz, N. (1997). Homologous recombination based modification in *Escherichia coli* and germline transmission in transgenic mice of a bacterial artificial chromosome. *Nat. Biotechnol.* 15, 859–865.

Accession Numbers

M10.1, M10.2, M10.3, M10.5, M10.7, M10.8, EC1-V2R, and EC2-V2R cDNA sequences were deposited in the GenBank database under accession numbers AY211078, AY211079, AY211080, AY211081, AY211082, AY211083, AJ543404, and AJ543405, respectively.